

Dolomite Geochemistry and Distribution in the Jurassic Samana Suk Formation, Salhad Section, Lesser Himalayas, North Pakistan

Syed Muhammad Wasim Sajjad*, Junaid Mehmood, Usman Said, Imran Ahmad, Ibrar Ul Haq, Salman Khurshid, Asad Muhammad

Department of Geology, University of Malakand, Chakdara, Dir Lower, Khyber Pakhtunkhwa, Pakistan

Received on February 3, 2024; Accepted on October 2, 2024

Abstract

The current study documents dolomites' occurrence, geometry, and distribution within the Middle Jurassic Samana Suk Formation, Salhad Section, Southern Hazara Basin of Lesser Himalayas, Northern Pakistan. Field observations in conjunction with petrographic and geochemical investigations revealed that the host limestone is diagenetically modified by various dolomitization phases. During field studies, it has been noticed that 75% of the lithology of the studied formation is unaltered limestone, while 25% has been dolomitized. The limestone is mostly light grey and oolitic while dolomite exhibits dark grey color. The diagenetic features observed in the field include stylolite, fractures, and calcite veins. Petrographic examination illustrates that the mud-dominated facies are more susceptible to dolomitization while the grainstone facies show resistance due to the earlier pore-filling marine cementation. The dolomites were classified into coarsely crystalline euhedral dolomites (DI), medium to coarse crystalline euhedral zoned dolomites (DII), and coarsely crystalline anhedral dolomites (DIII). These dolomites' carbon and oxygen isotope values range from +0.88‰ to +1.71‰ V-PDB and -2.98‰ to -6.84‰ V-PDB respectively. The highly depleted stable C & O isotopic signatures of different dolomites show significant deviation from original marine Middle Jurassic signatures (-8.87 to -4.47‰ V-PDB) and suggest multiphase dolomitization events.

© 2024 Jordan Journal of Earth and Environmental Sciences. All rights reserved

Keywords: Petrography, Diagenesis, Samana Suk Formation, C & O -Isotopes, Dolomitization, North Pakistan

1. Introduction

Carbonate rocks are a class of sedimentary rocks that primarily comprise (>50%) of carbonate minerals and are broadly categorized into two types: limestone and dolostone. Limestones are considered the principal carbonate rocks that consist of the mineral calcite and/or aragonite. They have similar CaCO_3 composition with different crystal structures, i.e., calcite is trigonal while aragonite is orthorhombic (Bell, 2016). Aragonite is metastable and readily converted into low magnesium calcite with time by losing magnesium (Flügel and Flügel, 2004). Therefore, calcite and, to a lesser extent, dolomite are regarded as the major constituent of carbonate rocks (Flügel and Flügel, 2004). Dolostone is a carbonate rock that is predominantly comprised of mineral dolomite, induced by the secondary alteration or replacement of limestone during diagenesis. Diagenesis includes all the physical, chemical, and biological changes that the sediments undergo from the moment of deposition till before the domain of metamorphism (Tucker and Bathurst, 2009). The major processes, involved in carbonate diagenesis, are dissolution, cementation, lithification, alteration, bacterial action, and soft sediment deformations (Tucker and Bathurst, 2009). These diagenetic alterations are mainly controlled by the depositional environments which include marine, meteoric, and burial diagenesis (Purdy, 1968; Tucker and Bathurst, 2009; Abed et al., 2023). In recent decades, many researchers have focused on the dolomitization since the

dolomite reservoirs have great hydrocarbon potential (Azmy et al., 2001; Swart et al., 2005; Azmy et al., 2008; Jiang et al., 2014; Jiang et al., 2016; Jiang et al., 2019; Liu et al., 2020; Zhemchugova et al., 2020; Xu et al., 2021). During the dolomitization event, the net calcite dissolution contributes to the porosity enhancement (Tucker and Wright, 1990; Tucker, 1993). The current study aims to investigate the distribution of dolomites and dolomitization process that occur in the Jurassic Samana Suk Limestone from Lower Salhad area, Abbottabad, Pakistan. It is the first study of their own kind, and previously no such detailed work has been carried out in the area.

2. Previous Studies

The carbonates of the Jurassic Samana Suk Formation exposed in Salhad area, Abbottabad Pakistan, have also been dolomitized which was not yet studied. Previously, different authors worked on and highlighted the important aspects of the Jurassic Samana Suk Formation from the Indus Basin, Trans-Indus Ranges, Kohat Ranges, Samana Ranges, and Kala Chitta Ranges. Shah et al., (2016 and 2020) studied the dolomitization and the effect of dolomitization on the reservoir quality of Samana Suk formation from Margalla Hill Ranges and Southern Hazara Basin. Rahim et al., (2020 and 2022) analyzed the various diagenetic and dolomitization events of Samana Suk Formation from the Himalayan Foreland Basin. Khan et al., (2021 and 2022) focused on the

* Corresponding author e-mail: geowaseem777@yahoo.com

diagenetic alteration of Jurassic carbonates from the Kohat Ranges. The sedimentological, sequence stratigraphic, and diagenetic alteration and their effect on reservoir properties of the Samana Suk Formation have been focused on by many researchers in several previous studies (Khan et al., 2020; Nizami and Sheikh, 2020; Rahim et al., 2020; Sajjad et al., 2020; Saboor et al., 2020; Wadood et al., 2021; Qamar et al., 2023; Ali et al., 2023; Khan et al., 2024). Miraj et al., (2021) and Shah et al., (2021) studied the marine deposits of the Samana Suk Formation in terms of source rock evaluation from the Middle Indus Basin and Punjab Platform, Pakistan.

3. Geological Setting

The youngest single supercontinent Pangea was initially comprised of all the earth landmasses. About 220Ma, the Pangea broke up into the Northern Laurasia and Southern Gondwana landmasses (Le Pichon et al., 2022). The present-day North America and Eurasia occupied Laurasia, while India, along with the current southern hemisphere continents, was originally part of the Southern Gondwana land (Plummer et al., 2016). Almost 167 million years ago, the Indian plate started to break up and subsequently fragmented from Gondwana, East Gondwana, Madagascar, Seychelles and moved toward northern hemisphere (Chatterjee and Scotese, 1999; Bandyopadhyay et al., 2010). The Indian continental breakup from Gondwana (~167 Ma) till its collisional orogeny with Asia during Eocene (~50 Ma) represents the longest journey 9000 km in 160 million years (Dietz and Holden 1970; Chatterjee 1992; Chatterjee and Scotese 2010; Chatterjee et al., 2013). This journey started from continental breakup followed by northward continental drifting, sea floor spreading, new ocean formations, volcanisms, fault systems, continental and oceanic subduction, continental collision, accretion, and mountain building process (Chatterjee et al., 2013). The collisional orogeny of Indian and Eurasian plate gives rise to the formation of Himalayas and Himalayan fold and thrust belt system (Klootwijk et al., 1992; Searle et al., 1997; Hussain et al., 2020). The study identified the northwestern part of Hazara Kashmir Syntaxis (Figure 1), situated in the lesser Himalayas of Pakistan (Yeats and Hussain, 1987). The study area is bound by the Panjal Thrust toward NNW while Nathia Gali Thrust marks the SSE boundary (Figure 1).

The stratigraphy of the area comprises Precambrian, Precambrian to early Cambrian, and Jurassic to Cretaceous rock sequences (Figure 2). The distribution, nomenclatures, thickness, and revised stratigraphy of the area are still under consideration, but here in this study, we follow the stratigraphy of Pakistan approved by the Stratigraphic Committee of Pakistan (Shah, 1977). The Hazara and Tawanal Formation represents the Precambrian sequence. Lithologically, the Hazara Formation dominantly comprises slate, while the Tanawal Formation is composed of quartzose schist (Calkins et al., 1975).

Abbottabad Formation and Hazira Formation represent the early Cambrian rock units of the area. The Abbottabad formation comprises the dolomites and sandstone lithology (Shah, 1977). The Hazira Formation is composed of the mudstone, siltstone, and sandstone (Shah, 1977). The

Jurassic and Cretaceous rock sequence, exposed in the study area, includes the Samana Suk, Chichali, Lumshiwai, and Kawagarh Formations (Shah, 1977). The name Samana Suk Formation is derived from the type section Samana Ranges where a 365m thick outcrop is well exposed (Iqbal and Shah, 1980). The formation is comprised of bedded limestone, fossiliferous limestone, oolitic limestone, ferruginous sandy limestone, dolomites, and calcareous sandstone. In the study area, the lower contact of the formation is unconformable with the Hazira Formation (Figure 2), while the upper layer has a conformable contact with the Chichali Formation (Shah, 1977; Naka et al., 1996). From the well-preserved macro and microfossils, the formation has been assigned to the Middle Jurassic age (Fatmi, 1977). The Chichali and Lumshiwai Formations generally comprise glauconitic sandstone shale and minor phosphorite and glauconitic sandy mudstone. The Late Cretaceous Kawagarh Formation is composed of thick to thin-bedded limestone, sandstone, and dolomites. In the field, it is very difficult to differentiate the Samana Suk Formation from Kawagarh Formation. However, it can be easily differentiated through the diagnostic oolitic limestone bed of Samana Suk Formation which is completely absent in the Kawagarh Formation (Naka et al., 1996).

4. Methodology

4.1 Field Work

The 35-meter-thick Salhad section is located on the Hazara Motorway along the Silk Route Salhad, Abbottabad. The section was traced and measured. The limestone and dolomite were differentiated through 10% dilute HCl and other field features like clear color contrast and Butcher Chop Weathering. In the study area, the Samana Suk Formation was identified by the presence of diagnostic oolitic limestone. Twenty samples were collected from limestone and dolomite for thin section and stable isotope analysis.

4.2 Laboratory Work

The collected samples were cut through a rock cutting machine in the thin-section laboratory of the National Centre of Excellence in Geology (NCEG), Peshawar University, Pakistan. The slabs were polished and marked for thin section preparation. Fifteen representative thin sections were prepared which were then studied by using a conventional microscope (NIKON LV100ND with 5 megapixels digital camera) in the petrographic lab of NCEG, University of Peshawar. The detailed petrography includes crystal morphology, size and textures, dolomite sizes, textures and their relationships with matrix, and various cement types.

4.3 Stable Isotope Analysis

Based on field investigation and petrographic observations, the different dolomite phases were analyzed for stable oxygen ($\delta^{18}\text{O}$) and carbon isotopes ($\delta^{13}\text{C}$). For $\delta^{18}\text{O}$ & $\delta^{13}\text{C}$ isotopes analysis, rocks powdering of different phases were carried out. During the powdering process, caution was followed to avoid contamination. A total of nine samples from different dolomite phases were first micro drilled (up to 2 grams) by using a hand-held dental driller and were packed in a sample holder tube. The dolomite samples were further analyzed for stable oxygen ($\delta^{18}\text{O}$) and carbon isotopic ($\delta^{13}\text{C}$) isotopes in the Isotope Application Division of PINSTECH,

Islamabad, Pakistan. The obtained results were presented as per mill (‰) relative to Vienna Pee Dee Belemnite (V-PDB). The stable isotope analyses were performed by using the proposed digestion method, via reacting the carbonate powder with 100 percent phosphoric acid having density lesser than 1.9 under a temperature of 75 °C in Carbo Kiel single sample acid bath coupled to a Finnigan-M.A.T 252 mass-spectrometer apparatus. As a result of carbonate powder

digestion CO₂ gas is produced from which the ratio 18O & 16O and 13C & 12C were restrained. The stable isotopic results are designated in per mill (‰) relative to (V-PDB) via allocating a δ13C range of +1.95‰ & δ18O ranging from -2.20‰ to NBS 19. In dolomite, the composition of oxygen isotopic results are revised through a fractional process provided by (Rosenbaum & Sheppard, 1986).

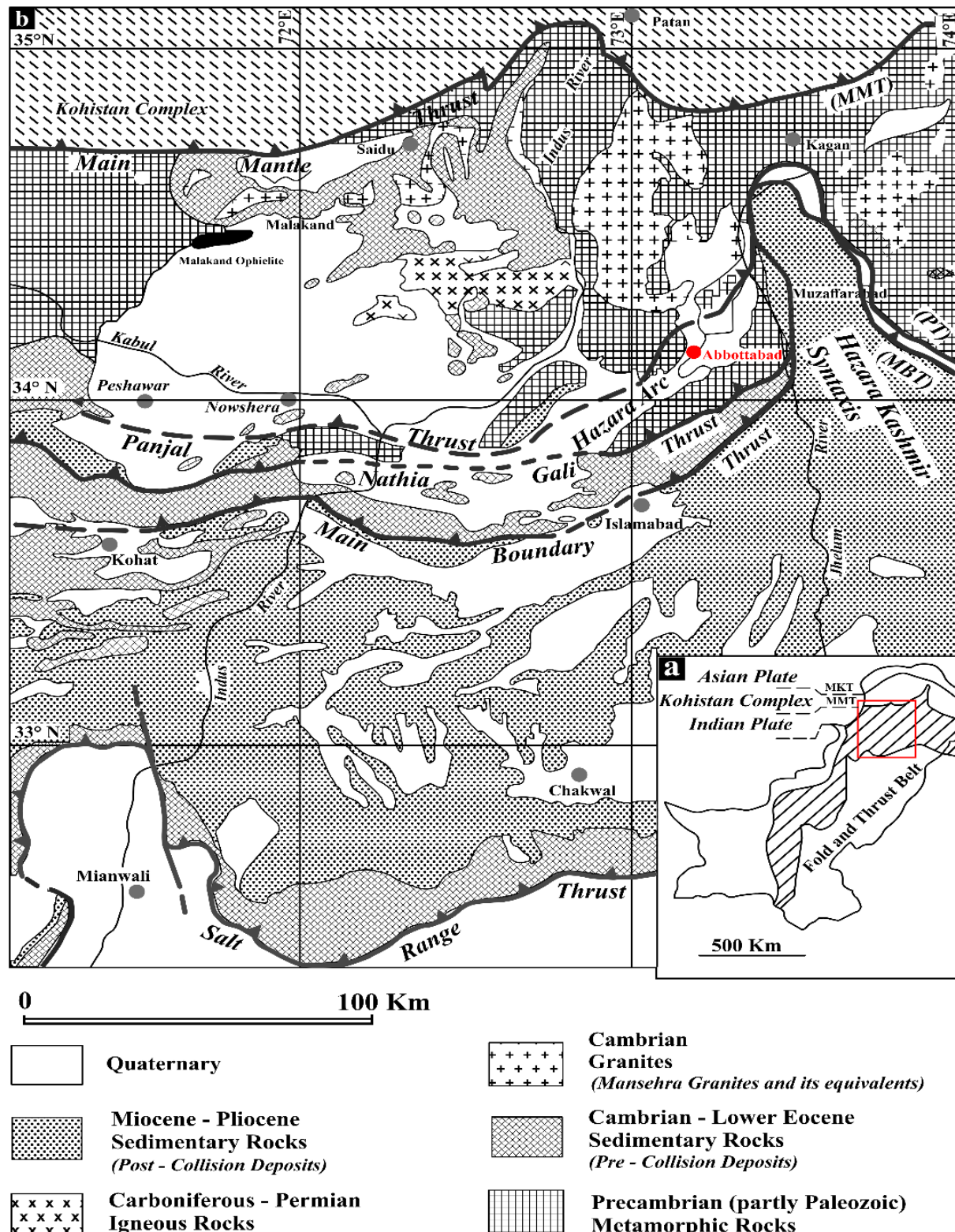


Figure 1. (a) A generalized tectonic map of Pakistan showing the Himalayan fold and thrust belt. The red box shows the study area in the Figure. (b) Geological map of Northern Pakistan illustrates major thrusts. The red solid circle shows the location of the study area (Hylland et al., 1988; Qureshi et al., 1993; Naka et al., 1996).

5. Results

5.1 Field Observations

The Salhad section of Samana Suk Formation comprises limestone and dolomite beds (Figure 3). The limestone is differentiated from dolomite through clear color contrast and a 10% dilute HCL test. In the area, the lower contact of the Samana Suk Formation is the Cambrian Hazira Formation (Figure 3b). The Samana Suk Formation comprises the diagnostic oolitic limestone bed showing a sharp contact with dark grey dolomite (Figure 3c). The formation also comprises the golden dolomites that usually fill veins and fractures (Figure 3d). Bedding parallel stylolite (BPS) is also observed (Figure 3e).

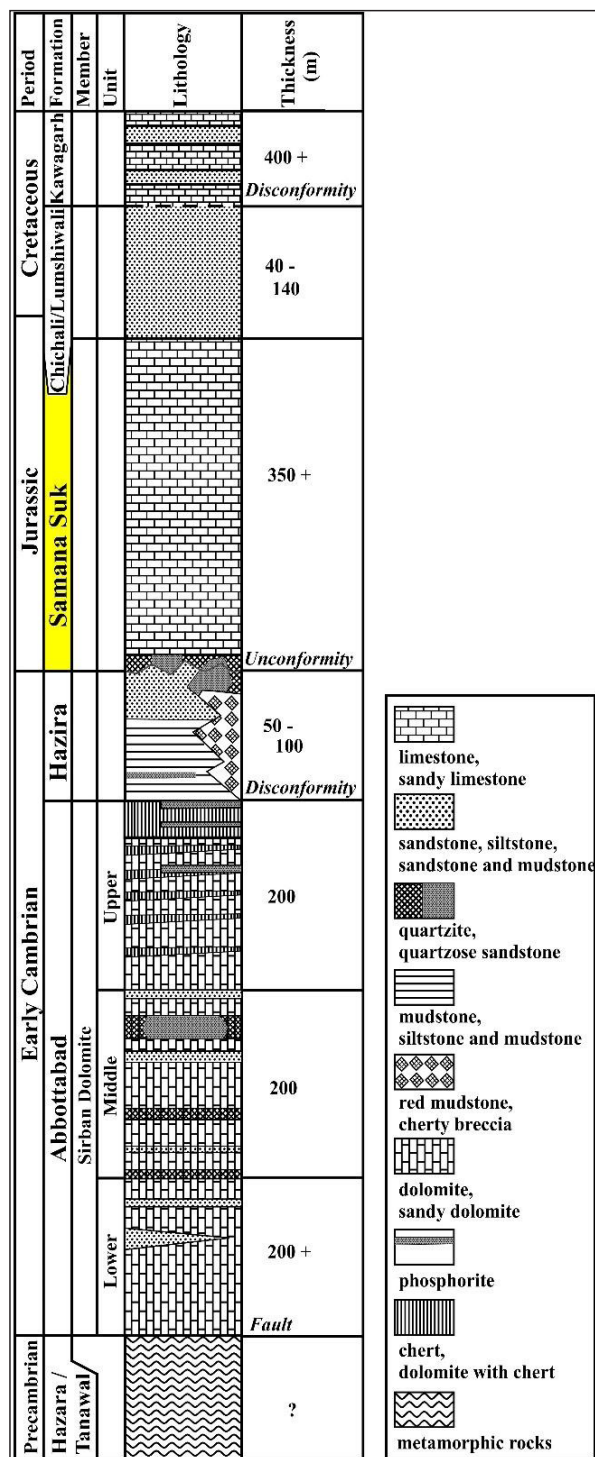


Figure 2. Generalized stratigraphic column of the study area Abbottabad. The current study is carried out on the Jurassic Samana Suk Formation which is highlighted by yellow color.

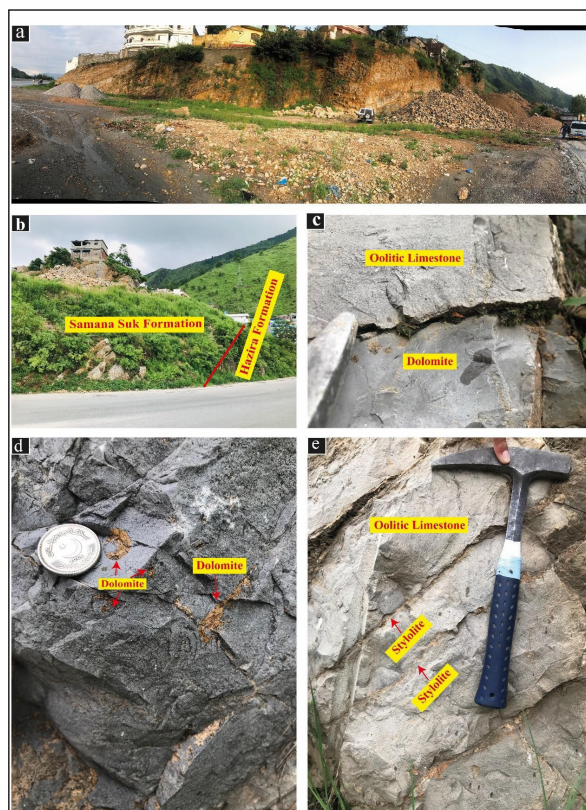


Figure 3. Field photographs (a) Panoramic view of the Jurassic Samana Suk Formation, Salhad Section, Abbottabad (b) Lower contact of Jurassic Samana Suk Formation with Cambrian Hazira Formation. (c) Sharp contact between the light grey oolitic limestone and dark grey dolomite. (d) Arrow indicating the occurrence of golden colour dolomites along vugs and fractures. (e) Arrow showing low to high amplitude bedding parallel stylolites.

5.2 Petrography

Based on field observations and microscopic examination, host limestone and different dolomite types were recognized within the Salhad section. The current study is not considered to show the entire petrographic details but only presents the diagenetic alterations that are important to the objectives of this paper. The detailed work on the limestone petrography was previously carried out by Ullah et al., (2016) and recognized five microfacies including Bioclastic Grainstone, Bioclastic Ooidal Peloidal Packstone, Siliciclastic Bioclastic Wackestone, and Peloidal Mudstone. The petrographic study shows that the limestone underwent through a complex diagenetic alteration i.e., dolomitization which was studied here in detail. During petrography, different dolomite types were recognized by using Sibley and Gregg's dolomite classification scheme (1987). Three replacive matrix dolomite types: coarse grain euhedral dolomite (DI), medium to coarse grain euhedral zoned dolomite (DII), and coarse grain anhedral dolomite (DIII), were recognized (Figure 4 and 5). The replacive matrix dolomite DI is characterized by their equigranular crystals and shows a crystal size up to 250 μm (Figure 4c and d). This type of dolomites mostly possesses euhedral shape having cloudy appearance and clear oval crystal rims (Figure 4c and d). DI mostly occurs in association with micrite and sparite of host limestone (Figure 4c and d). It doesn't show any significant occurrence and is present all about 5% of the total host rock volume (Figure 4c and d).

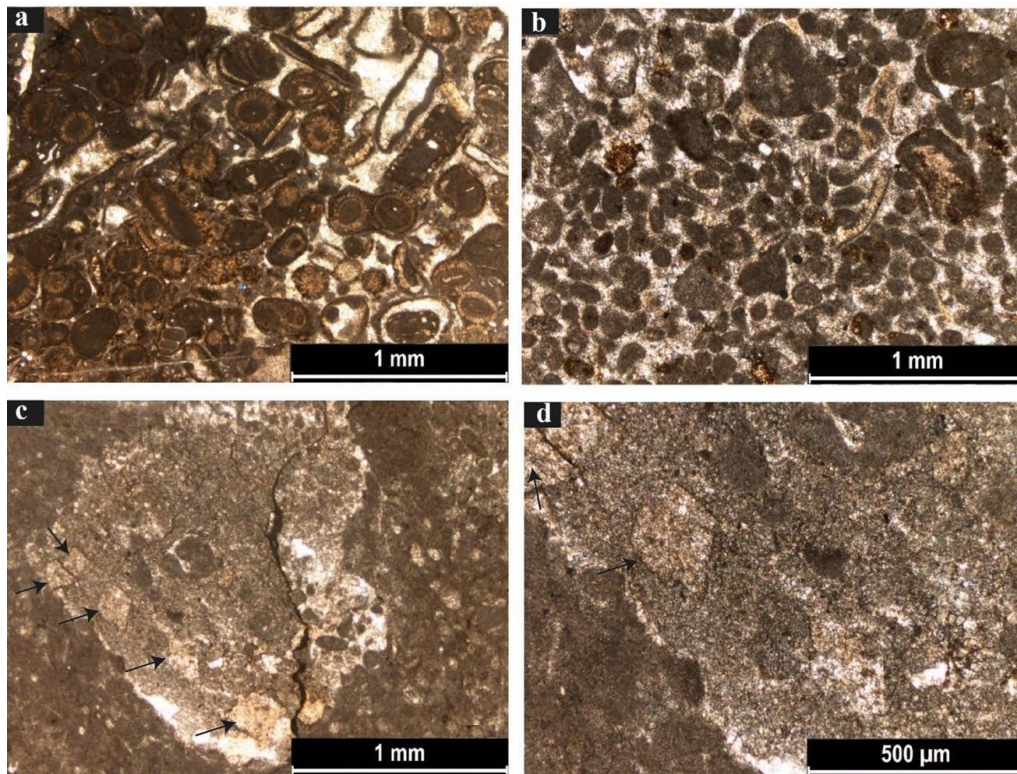


Figure 4. Photomicrographs showing (a and b) peloidal grain-stone microfacies which shows resistance to dolomitization event. (c and d) arrows indicate coarse crystalline euhedral dolomites (DI), representing the first stage of multiphase dolomitization events.

DII is the second type of replacive matrix dolomite which is characterized by its euhedral shape, having perfectly rhombohedral successive zones (Figure 5a and b). This type of dolomite shows minor to densely packing and preserved the original limestone texture (Figure 5a and b). The dolomite DII shows inequigranular crystals of euhedral shape with alternate cloudy and clear crystal bands (Figure 5a and b).

These dolomites commonly infill the veins and fractures (Figure 3d and 5b). The dolomite DIII is characterized by its non-planar anhedral crystal shapes (Figure 5c and d). This type of dolomite shows densely packing, inequigranular size and is completely diminishing the original texture of host limestone (Figure 5c and d).

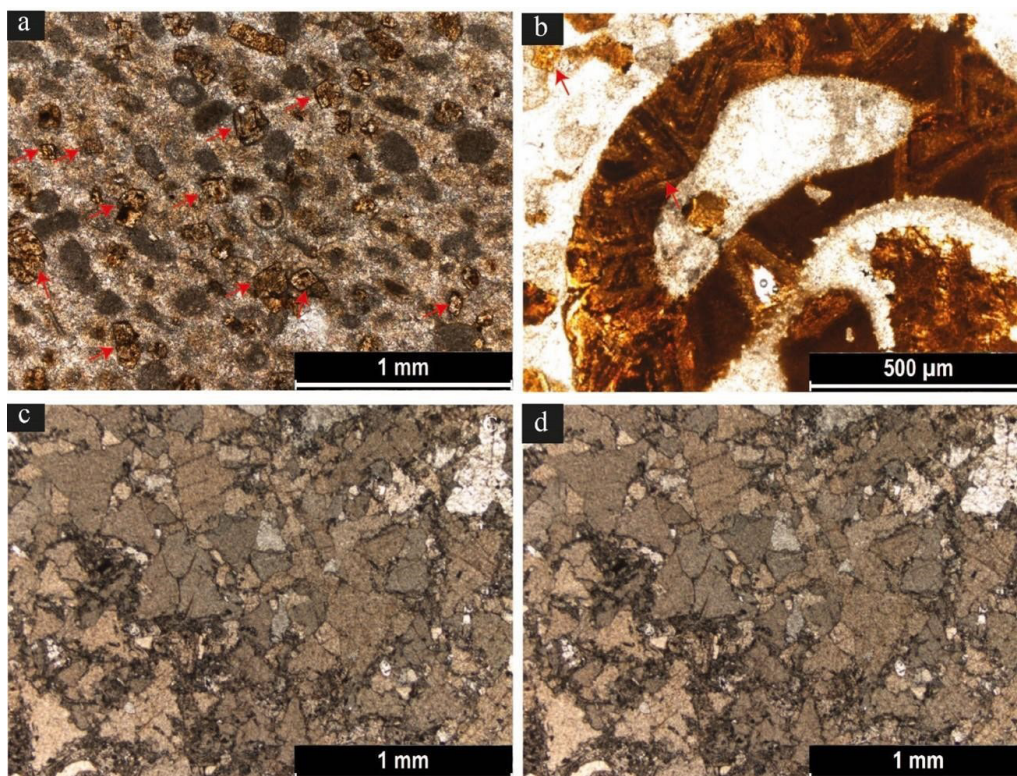


Figure 5. Photomicrographs of dolomite phases. (a) Medium to coarse crystalline euhedral zoned dolomites DII. (b) The dolomite DII filling the weak zones and void spaces of host limestone which occurs as a void filling. (c and d) later stage coarse crystalline anhedral dolomites DIII.

5.3 Stable Carbon and Oxygen Isotope analysis

Nine representative samples from dolomites were analyzed for stable carbon and oxygen isotopes ($\delta^{13}\text{C}$ and $\delta^{18}\text{O}$). The $\delta^{13}\text{C}$ and $\delta^{18}\text{O}$ values of these dolomites are listed in Table 1. The obtained results were then compared with the original Jurassic Marine (sea) carbonate signatures of Fursich et al., (2004). The dolomite DI hold $\delta^{18}\text{O}$ values in the range of -2.98‰ and -3.94‰ V-PDB while the $\delta^{13}\text{C}$ values varies from +1.32‰ to +1.53‰ V-PDB. The $\delta^{18}\text{O}$ and $\delta^{13}\text{C}$ results of DII varies from -4.89‰ to -5.37‰ V-PDB and +0.88‰ to +1.32‰ V-PDB respectively. The dolomite DIII exhibit $\delta^{18}\text{O}$ signatures in the range of -6.11‰ and -6.84‰ V-PDB while the $\delta^{13}\text{C}$ values varies from +1.19‰ to +1.46‰ V-PDB. All the obtained results were then compared with the known Middle Jurassic original sea water values which range from -2.8‰ to -1.8‰ $\delta^{18}\text{O}$ V-PDB and +0.0‰ to +1.8‰ $\delta^{13}\text{C}$ V-PDB (Fursich et al., 2004, Khan et al., 2021).

Table 1. The stable carbon and oxygen isotope values of the dolomite phases from the Jurassic Samana Suk Formation

Sr. No	Sample Code	Dolomite Types	$\delta^{13}\text{C}$ V-PDB	$\delta^{18}\text{O}$ V-PDB
01	JSS 3	DI	+1.35	-3.94
02	JSS 4A	DI	+1.53	-3.63
03	JSS 6	DI	+1.32	-2.98
04	JSS 10	DII	+0.88	-4.89
05	JSS 13	DII	+1.11	-5.37
06	JSS 14A1	DII	+1.71	-5.16
07	JSS 16	DIII	+1.46	-6.11
08	JSS 17A1	DIII	+1.41	-6.47
09	JSS 18	DIII	+1.19	-6.84

6. Discussions

The Jurassic Samana Suk Formation is composed of carbonates assemblage which represents a typical Mesozoic succession that attracts the interest of many researchers. The formation comprises oolitic, pelitic and fossiliferous limestone that are deposited in the inner to middle shelf environment during Jurassic (Qureshi et al., 2008; Nizami and Sheikh, 2009; Hussain et al., 2013; Rahim et al., 2020). In the study area, after their deposition, the formation passes through various diagenetic phases like micritization, neomorphism, compaction, recrystallization, cementations, and dolomitization (Ullah et al., 2016). In the current study, the process of dolomitization is investigated in detail in terms of field observations, petrography, and stable isotope analysis. According to Ullah et al., (2016), the micritization occurs most commonly as a micritic rim around skeletal and non-skeletal grains and represents the early marine diagenetic phase (Tucker and Wright, 1990). It is also reported by Rahim et al., (2020) and Khan et al., (2022) in the Jurassic Samana Suk Formation from Himalayan Hill Ranges and Kohat Basin respectively. In the field observations, the early diagenesis is observed in the form of mechanical and chemical compaction (Figure 3d and e). During shallow to deep burial conditions, the overburdened depositional pressure which combines with the tectonic stresses creates various fractures (Ahmad et al., 2017; Rahim et al., 2020). The mechanical compaction starts soon after the

initial few meters of burial conditions (Shinn and Robbin, 1983). Based on its peaks (tooths), the stylolites are either bedding parallel (horizontal peaks) or bedding perpendicular (vertical peaks). Vertical peak stylolites are when the peak direction is vertical and perpendicular to bedding planes. Horizontal peak stylolites are defined where the peak (teeth) direction is horizontal and parallel to bedding planes (Al-Hejoj et al., 2013). The bedding parallel stylolites (Figure 3e) are induced through the pressure dissolution process of chemical compaction (Lloyd, 1977; Alhejoj et al., 2018; Khan et al., 2022). The mechanical and physical compaction most occurred in Samana Suk Formation which is observed and reported by many authors (Shah et al., 2016; Khan et al., 2020; Rahim et al., 2020; Shah et al., 2020; Wadood et al., 2021; Khan et al., 2021 and 2022; Rahim et al., 2022). This early diagenetic episode is followed by the formation of various dolomites representing later diagenetic phases. The fractures and voids are filled by the later diagenetic golden color dolomite (Figure 3d). The dark grey color of dolomite shows a sharp contact with the oolitic limestone (Figure 3c) suggesting a later dolomitization event (Rahim et al., 2022).

Petrographically, the dolomites were classified into three types following Sibley and Gregg's (1987) classification. These various dolomite texture shows the occurrences of multiphase dolomitization events (Khan et al., 2020). The dolomite (DI) exhibits a planar euhedral crystal shape which perceives their formation at near-surface conditions (Sibley 1982; Rahim et al., 2020). The coarser rhomb of dolomite DI shows clear crystal boundaries (Figure 4c and d) and represents the earlier dolomitization stage, replacing the matrix and grains of precursor limestone. The formation of coarser grain euhedral dolomite DI originates from shallow burial conditions of later diagenetic event (Amthor et al., 1991; Khan et al., 2020). Contrary to dolomite DI, the dolomite DII shows planar euhedral crystals and coarser grains that fill the vugs and fractures of host limestone (Figure 5a and b) which endorsed their precipitation from hot saline brines with temperature more than 60°C of deep burial regime (Al-Aasm et al., 2002; Shembilu et al., 2021; Liang et al., 2022). The occurrence of dolomites along stylolites and fractures indicates that the fractures provide a possible pathway for these dolomitizing fluids (Martín-Martín et al., 2017; Rahim et al., 2020). DII is zoned dolomite which attributes their origin from hydrothermal fluids (Gregg and Shelton, 1990; Warren, 2000; Rahim et al., 2022). According to Gao et al., (2016), the concentric zones of dolomites are for the reason of their burial origin. Such kind of zoned dolomite of the same kind and nature has been reported regionally and locally (Drivet and Mountjoy, 1997; Al-Aasm and Packard, 2000; Chen et al., 2004; Azmy et al., 2009; Conliffe et al., 2012; Rott and Qing, 2013; Khan et al., 2020; Shah et al., 2020; Khan et al., 2022). The DIII is coarse-grained anhedral dolomite showing tight packing and more curved faces (Figure 5c and d) which shows a rapid growth rate at higher temperatures (Montañez and Read, 1992; Al-Aasm and Packard, 2000; Warren, 2000; Huang et al., 2003; Machel, 2004; Khan et al., 2022; Saleem et al., 2022; Saleema et al., 2022).

The results $\delta^{13}\text{C}$ and $\delta^{18}\text{O}$ were cross-plotted and compared with the known original Jurassic marine signatures of $\delta^{13}\text{C}$ and $\delta^{18}\text{O}$ varies from +0.0% to +1.8% (V-PDB) and from -2.8% to -1.8% (V-PDB) respectively (Figure 6; Fürsich et al., 2004; Khan et al., 2021). The $\delta^{18}\text{O}$ values of three dolomite types lie between -6.88 and -2.98 which are very lighter and depleted from original Jurassic marine signature and are consistent with multiphase dolomitization events (Dickson and Coleman, 1980; Swart, 2015; Rahim et al., 2020; Khan et al., 2021; Saleem et al., 2022;). The lighter $\delta^{18}\text{O}$ values indicate to rock fluids interaction where the fluid temperature is higher than the ambient temperature of precursor limestone (Shah et al., 2016; Khan et al., 2021). The $\delta^{18}\text{O}$ values of dolomite DI range between -2.98 and -3-94 ‰ V-PDB (Table 1 and Figure 6) which show relatively less depletion and mark the earlier phase of dolomitization event of low temperature (Sibley and Gregg, 1987; Gregg and Shelton, 1990; Shah et al., 2019). In contrast, the dolomite DII represents more depleted $\delta^{18}\text{O}$ values (Table 1 and Figure 6) and represents relative burial and high temperature for their formation. The occurrence of dolomite DII along fractures, its zoned crystals, and depleted $\delta^{18}\text{O}$ values represents its formation during burial conditions from hydrothermal fluid interactions (Gregg and Shelton, 1990; Warren, 2000; Al-Aasm et al., 2002; Gao et al., 2016; Martín-Martín et al., 2017; Rahim et al., 2020; Shembilu et al., 2021; Liang et al., 2022). Among all the observed dolomite phases, the dolomite DIII shows more depleted $\delta^{18}\text{O}$ signatures from standard marine values (Table 1 and Figure 6) and endorsed a later diagenetic hydrothermal origin (Sibley and Gregg, 1987; Allan and Wiggins, 1993; Moore, 2001; Shah et al., 2019).

The current isotope results were also compared with previous published isotope values of various dolomite types of the Samana Suk Formation (Figure 6b). The isotope values of the current section show consistency with the isotope values from different reported sections of the Samana Suk Formation (Figure 6b). More information is available in Figure 6. Moreover, in the current study, the packstone and grainstone facies are not affected by dolomitization events since the pore spaces and conduit for hydrothermal fluids have already been occupied by the calcite cements (Figure 4a and b). These grain-supported facies have negligible porosity and don't allow dolomitization fluids to pass and cause dolomitizations, while the wackestone and mudstone units shows minute primary porosity and permeability and show resistance to significant calcite cementation during earlier diagenetic processes. These facies possess intergranular pore-network which were the target zones for Mg-rich fluids during dolomitization process. Same grainstone, and packstone facies show resistance to dolomitization and mudstone, and wackestone facies underwent through dolomitization process in the Samana Suk Formation were reported by many authors (Rahim et al., 2020; Shah et al., 2020; Khan et al., 2020; Saboor et al., 2020; Khan et al., 2022).

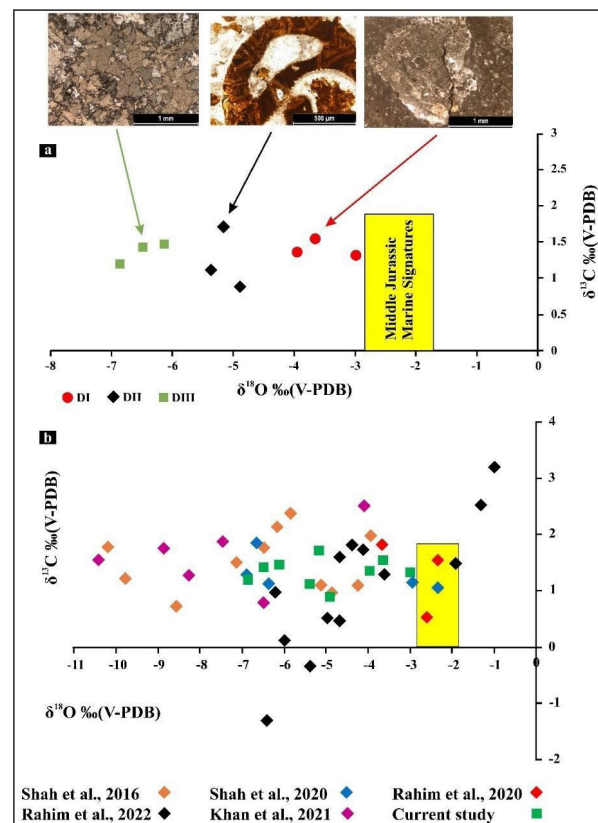


Figure 6. Cross plots between $\delta^{13}\text{C}$ and $\delta^{18}\text{O}$ (V-PDB) values representing various dolomite phases of Jurassic Samana Suk Formation which are compared with the known Middle Jurassic marine seawater signatures after Fürsich et al., (2004). (a) Various dolomites phases showing depletion from original marine condition. (b) The result of the current study is compared with previously reported data. The data distribution documents the progressive depletion of isotopic composition from the known Jurassic marine sea water signatures. Note that the value of the current study shows consistency with the published data.

7. Conclusions

The Jurassic Samana Suk Formation is characterized by a thick carbonate sequence which passes through various diagenetic alteration. The diagenetic modification is traced by means of field observation, petrography, and stable isotopes analysis. From this study, it is concluded that a multiphase dolomitization processes occur in the Samana Suk Formation. Soon after the deposition, the first phase of dolomitization initiated which is supported by the occurrence of stylolite and less depleted $\delta^{18}\text{O}$ values. It is followed by the second phase of dolomitization along vugs and fractures which is supported through more depleted $\delta^{18}\text{O}$ values and dolomite zonation. The fractures act a conduit for Mg-rich hydrothermal fluids. The third phase of dolomitization is marked by the presence of coarse grained, curved face anhedral dolomites showing a very depleted $\delta^{18}\text{O}$ values from standard marine signatures. The more depleted $\delta^{18}\text{O}$ values suggest their formation from hydrothermal fluids. The study area lies in the Himalayan orogeny where the MBT mark the southern boundary. The fractures and various small and larger faults, resulted due to Himalayan orogeny, may provide as possible pathway for these Mg-rich hydrothermal fluids.

Acknowledgments

We would like to express our sincere appreciation to the National Centre of Excellence in Geology (NCEG), University of Peshawar for access to their petrographic lab.

References

- Abed, A.M., Al-Halboosi, J.M., Al-Jibouri, A.S., Al-Hetty, S.O. (2023). 2D Seismic Stratigraphic Analysis of Harthaand Kifl Formations in Balad Area–Center of Iraq. *Jordan Journal of Earth & Environmental Sciences*, 14(1).
- Al-Aasm, I.S., Lonnee, J., Clarke, J. (2002). Multiple fluid flow events and the formation of saddle dolomite: case studies from the Middle Devonian of the Western Canada Sedimentary Basin. *Marine and Petroleum Geology*, 19(3): 209-217.
- Al-Aasm, I.S., Packard, J.J. (2000). Stabilization of early-formed dolomite: a tale of divergence from two Mississippian dolomites. *Sedimentary geology*, 131(3-4): 97-108.
- Alhejoj, I., Alqudah, M., Alzughoul, K., Tarawneh, A. (2018). Post-Cretaceous Mesostructures and Their Formation Mechanisms, Jordan. *Jordan Journal of Earth and Environmental Sciences*, 9(2).
- Al-Hejoj, I.K., Salameh, E., Abu Hamad, A. (2013). Deformed fossils and related structures in Jordan. *Jordan J. Earth Environ. Sci*, 5(1), 31-44.
- Allan, J.R., Wiggins, W.D. (1993). Dolomite reservoirs: Geochemical techniques for evaluating origin and distribution. *American Association of Petroleum Geologists*.
- Azmy, K., Knight, I., Lavoie, D., Chi, G. (2009). Origin of dolomites in the Boat Harbour Formation, St. George Group, in western Newfoundland, Canada: implications for porosity development. *Bulletin of Canadian Petroleum Geology*, 57(1): 81-104.
- Azmy, K., Lavoie, D., Knight, I., Chi, G. (2008). Dolomitization of the Lower Ordovician Aguathuna Formation carbonates, Port au Port Peninsula, western Newfoundland, Canada: implications for a hydrocarbon reservoir. *Canadian Journal of Earth Sciences*, 45(7): 795-813.
- Azmy, K., Veizer, J., Misi, A., de Oliveira, T.F., Sanches, A.L., Dardenne, M.A. (2001). Dolomitization and isotope stratigraphy of the vazante formation, sao francisco basin, Brazil. *Precambrian Research*, 112 (3-4): 303–329.
- Bandyopadhyay, S., Chatterjee, S., Scotese, C. (2010). The wandering Indian plate and its changing biogeography during the Late Cretaceous–Early Tertiary period. *New aspects of Mesozoic biodiversity* 105-126.
- Bell, F.G. (2016). *Fundamentals of engineering geology*, Elsevier.
- Calkins, J.A., T.W.O., S.K.M. A. (1975). Geology of the southern Himalaya in Hazara, Pakistan and adjacent areas.
- Chatterjee, S. (1992). A kinematic model for the evolution of the Indian plate since the Late Jurassic. *New concepts in global tectonics*, 33-62.
- Chatterjee, S., Goswami, A., Scotese, C.R. (2013). The longest voyage: Tectonic, magmatic, and paleoclimatic evolution of the Indian plate during its northward flight from Gondwana to Asia. *Gondwana Research* 23(1): 238-267.
- Chatterjee, S., Scotese, C.R. (1999). The breakup of Gondwana and the evolution and biogeography of the Indian plate. *Proceedings-Indian national science academy part A* 65(3): 397-426.
- Chatterjee, S., Scotese, C.R. (2007). Biogeography of the Mesozoic lepidosaurs on the wandering Indian plate, *Paleontologia: Cenários de Vida*, Editora Interciência. Rio de Janeiro 551-579.
- Chatterjee, S., Scotese, C.R. (2010). The wandering Indian plate and its changing biogeography during the Late Cretaceous–Early Tertiary period. In: Bandopadhyay, S. (Ed.), *New Aspects of Mesozoic Biogeography*. Springer-Verlag, Berlin Heidelberg, Germany, pp. 105–126.
- Chen, D., Qing, H., Yang, C. (2004). Multistage hydrothermal dolomites in the Middle Devonian (Givetian) carbonates from the Guilin area, South China. *Sedimentology* 51(5): 1029-1051.
- Conliffe, J., Azmy, K., Greene, M. (2012). Dolomitization of the lower Ordovician Catoche formation: Implications for hydrocarbon exploration in western Newfoundland. *Marine and Petroleum Geology* 30(1): 161-173.
- Dietz, R.S., Holden, J.C. (1970). The breakup of Pangaea, *Scientific American* 223(4): 30-41.
- Drivet, E., Mountjoy, E.W. (1997). Dolomitization of the Leduc Formation (Upper Devonian), southern Rimbey-Meadowbrook reef trend, Alberta. *Journal of Sedimentary Research* 67(3): 411-423.
- Flügel, E., Flügel, E. (2004). Diagenesis, porosity, and dolomitization. *Microfacies of carbonate rocks: Analysis, interpretation and application*, 267-338.
- Gregg, J.M., Shelton, K.L. (1990). Dolomitization and dolomite neomorphism in the back reef facies of the Bonnetterre and Davis formations (Cambrian), southeastern Missouri, *Journal of Sedimentary Research* 60(4): 549-562.
- Hou, M.C., Jiang, W.J., Xing, F.C., Xu, S.L., Liu, X.C., Xiao, C. (2016). Origin of dolomites in the Cambrian (upper 3rd-Furongian) formation, south-eastern Sichuan Basin, China. *Geofluids* 16(5): 856-876.
- Huang, S.J., Shi, H., Mao, X.D. (2003). Diagenetic alteration of earlier Palaeozoic marine carbonate and preservation for the information of sea water. *Journal of chengdu university of technology* 30(1): 9-18.
- Hussain, G., Fang, X., Usmani, N.A., Gardezi, S.A.H., Hussain, M., Asghar, H., Khalid, S. (2020). Structural and stratigraphic studies of Hazara-Kashmir Syntaxis, northwestern Himalaya, Pakistan, *North American Academic Research* 3(9): 1-14.
- Hylland, M.D., Riaz, Ahmad, S. (1988). Stratigraphy and structure of the southern Gandghar range, Pakistan, *Geological Bulletin University of Peshawar* 1: 15-24.
- Jiang, L., Cai, C.F., Wordern, R.H., Crowley, S.F., Jia, L., Zhang, K. (2016). Multiphase dolomitization of deeply buried Cambrian petroleum reservoirs, Tarim Basin, north-west China. *Sedimentology* 63(7): 2130–2157.
- Jiang, L., Worden, R.H., Cai, C., Li, K., Xiang, L., Cai, L., He, X. (2014). Dolomitization of gas reservoirs: the upper Permian Changxing and lower Triassic feixianguan formations, northeast Sichuan Basin, China. *Journal of Sedimentary Research* 84(10): 792-815.
- Jiang, L., Xu, Z., Shi, S., Liu, W. (2019). Multiphase dolomitization of a microbialite-dominated gas reservoir, the middle Triassic Leikoupo Formation, Sichuan Basin, China. *Journal of Petroleum Science and Engineering* 180: 820-834.
- Khan, E., Naseem, A.A., Khan, S., Wadood, B., Rehman, F., Saleem, M., Azeem, T. (2022). Facies Analysis, Sequence Stratigraphy and Diagenetic Studies of the Jurassic Carbonates of the Kohat Basin, Northwest Pakistan: Reservoir Implications. *Acta Geologica Sinica-English Edition* 96(5): 1673-1692.
- Khan, E.U., Naseem, A.A., Saleem, M., Rehman, F., Sajjad, S.W., Ahmad, W., Azeem, T. (2021). Petrography and geochemistry of dolomites of Samanasuk Formation, Dara Adam Khel Section, Kohat Ranges, Pakistan, *Sains Malaysiana* 50(11): 3205-3217.

- Khan, E.U., Saleem, M., Naseem, A.A., Ahmad, W., Yaseen, M., Khan, T.U. (2020). Microfacies analysis, diagenetic overprints, geochemistry, and reservoir quality of the Jurassic Samanasuk Formation at the Kahi Section, Nizampur Basin, NW Himalayas, Pakistan. *Carbonates and Evaporites* 35: 1-17.
- Khan, E.U., Saleem, M., Wasim Sajjad, S.M., Ahmad, Z., Javaid, Z. (2024). Reservoir heterogeneities due to diagenesis in Jurassic Samana Suk Formation Kahi section Nizampur Basin North West Himalayas Pakistan. *Acta Montanistica Slovaca*, 29(1).
- Klootwijk, C.T., Gee, J.S., Peirce, J.W., Smith, G.M., McFadden, P.L. (1992). An early India-Asia contact: paleomagnetic constraints from Ninetyeast ridge, ODP Leg 121. *Geology* 20(5): 395-398.
- Liang, J., Liu, S., Li, L., Dai, J., Li, X., Mou, C. (2022). Geochemical Constraints on the Hydrothermal Dolomitization of the Middle-Upper Cambrian Xixiangchi Formation in the Sichuan Basin, China. *Frontiers in Earth Science* 10: 927066.
- Liu, M., Xiong, Y., Xiong, C., Liu, Y., Liu, L., Xiao, D., Tan, X. (2020). Evolution of diagenetic system and its controls on the reservoir quality of pre-salt dolostone: The case of the Lower Ordovician Majiagou Formation in the central Ordos Basin, China. *Marine and Petroleum Geology* 122: 104-674.
- Machel, H.G. (2004). Concepts and models of dolomitization: a critical reappraisal, Geological Society, London, Special Publications 235(1): 7-63.
- Mahboubi, A., Nowrouzi, Z., Al-Aasm, I.S., Moussavi-Harami, R., Mahmudy-Gharaei, M.H. (2016). Dolomitization of the Silurian Niur Formation, Tabas block, east central Iran: Fluid flow and dolomite evolution. *Marine and Petroleum Geology* 77: 791-805.
- Miraj, M.A.F., Ali, A., Javaid, H., Rathore, P.W.S., Ahsan, N., Saleem, R.F., Malik, M.B. (2021). An integrated approach to evaluate the hydrocarbon potential of jurassic samana suk formation in Middle Indus basin, Pakistan. *Kuwait Journal of Science* 48(4).
- Montanez, I.P., Read, J.F. (1992). Fluid-rock Group (Lower Ordovician), US Appalachians. *Journal of Sedimentary Research* 62(5): 753-778.
- Moore, C.H. (2001). Diagenetic environments of porosity modification and tools for their recognition in the geologic record. Carbonate reservoirs porosity evolution and diagenesis in a sequence stratigraphic framework. *Developments in Sedimentology* 55: 61-88.
- Naka, T., Warrich, M.Y., Hirayama, J., Hassan, S. (1996). Stratigraphy, and structure of the Precambrian to Mesozoic, especially Precambrian (?) to Lower Cambrian phosphorite bearing formations in Abbottabad, northern Pakistan. *Bulletin-geological survey Japan* 47: 549-576.
- Nizami, A.R., Sheikh, R.A. (2010). Sedimentology of the middle Jurassic Samana Suk Formation, Makarwal section, Surghar Range, Trans Indus Ranges, Pakistan. *The Geological bulletin of the Punjab University* 44: 2009.
- Plummer, C.C., Carlson, D., Hammersley, L. (2016). *Physical geology*. McGraw-Hill/Education.
- Rahim, H.U., Qamar, S., Shah, M.M., Corbella, M., Martín-Martín, J.D., Janjuhah, H.T., Kontakiotis, G. (2022). Processes Associated with Multiphase Dolomitization and Other Related Diagenetic Events in the Jurassic Samana Suk Formation, Himalayan Foreland Basin, NW Pakistan. *Minerals* 12(10): 1320.
- Rahim, H.U., Shah, M.M., Corbella, M., Navarro-Ciurana, D. (2020). Diagenetic evolution and associated dolomitization events in the middle Jurassic Samana Suk Formation, Lesser Himalayan Hill Ranges, NW Pakistan. *Carbonates and Evaporites* 35: 1-26.
- Rahim, Y., Lia, Q., Jadoona, U.F., Lutfia, W., Khanb, J., Akhtar, S. (2020). Microfacies analysis of late Jurassic Samana Suk formation, Hazara basin lesser Himalaya north Pakistan. *Earth Sciences Malaysia (ESMY)* 4(2): 102-107.
- Rott, C.M., Qing, H. (2013). Early dolomitization and recrystallization in shallow marine carbonates, Mississippian Alida Beds, Williston Basin (Canada): evidence from petrography and isotope geochemistry. *Journal of Sedimentary Research* 83(11): 928-941.
- Saboor, A., Haneef, M., Hanif, M., Swati, M.A.F. (2020). Sedimentological attributes of the Middle Jurassic peloids-dominated carbonates of eastern Tethys, lesser Himalayas, Pakistan. *Carbonates and Evaporites* 35: 1-17.
- Sajjad, N.U.I. (2020). Microfacies Analysis and Depositional Environment of Middle Jurassic Samana Suk Formation, Chichali Nala Section, Surghar Range, Pakistan. *International Journal of Economic and Environmental Geology* 11(4): 00-00.
- Saleem, M., Rehman, F., Naseem, A.A., Khan, E., Sajjad, S.W., Ahmad, Z. (2022). Petrographic and geochemical characteristics of dolomites in the Devonian Shogram Formation, Karakorum Ranges, North Pakistan. *Current Science* 123(4): 583.
- Saleem, M., Sajjad, S.W., Khan, E.U., Naseem, A.A., Bangash, A.A., Rafique, A., Ahmad, W. (2022). Classification of the dolomites of Cretaceous Kawagarh formation in Hazara Basin North-west Himalayas Pakistan: evidence from field investigation, petrographic analysis and isotopic studies. *Carbonates and Evaporites* 37(1): 10.
- Saleema, M., Rehmana, F., Khana, E.U., Sajjada, S.W., Azeema, T., Jadoona, A., Naseema, A.A. (2022). Multiphase dolomitization in Devonian Shogram Formation, Chitral, Karakorum ranges, Pakistan: Evidence from outcrop analogue, petrography, and geochemistry. *Science Asia* 48(3).
- Searle, M., Corfield, R.I., Stephenson, B.E.N., McCarron, J.O.E. (1997). Structure of the North Indian continental margin in the Ladakh-Zaskar Himalayas: implications for the timing of obduction of the Spontang ophiolite, India-Asia collision and deformation events in the Himalaya. *Geological Magazine* 134(3): 297-316.
- Shah, M.M., Ahmed, W., Ahsan, N., Lisa, M. (2016). Fault-controlled, bedding-parallel dolomite in the middle Jurassic Samana Suk Formation in Margalla Hill Ranges, Khanpur area (North Pakistan): petrography, geochemistry, and petrophysical characteristics. *Arabian Journal of Geosciences* 9: 1-18.
- Shah, M.M., Rahim, H.U., Hassan, A., Mustafa, M.R., Ahmad, I. (2020). Facies control on selective dolomitization and its impact on reservoir heterogeneities in the Samana Suk Formation (middle Jurassic), Southern Hazara Basin (NW Himalaya, Pakistan): an outcrop analogue. *Geosciences Journal* 24: 295-314.
- Shah, S.B.A., Shah, S.H.A., Ahmed, A., Munir, M.N. (2021). Source Rock Potential of Chichali and Samana Suk Formations Deposits in Panjpir Oilfield Subsurface, Punjab Platform, Pakistan: Formation Deposits in Panjpir Oilfield Subsurface. *Pakistan Journal of Scientific & Industrial Research Series A: Physical Sciences* 64(1): 59-64.
- Shembilu, N., Azmy, K., Blamey, N. (2021). Origin of Middle-Upper Cambrian Dolomites in Eastern Laurentia: A Case Study from Belle Isle Strait, Western Newfoundland. *Marine and Petroleum Geology* 125: 104858.
- Sibley, D.F., Gregg, J.M. (1987). Classification of dolomite rock textures, *Journal of sedimentary Research* 57(6): 967-975.
- SM, I.S. (1977) Stratigraphy of Pakistan. Geological Survey of Pakistan Memoir, 12: 1-138.
- Swart, P.K., Cantrell, D.L., Westphal, H., Handford, C.R., Kendall, C.G. (2005). Origin of dolomite in the Arab-D reservoir from the Ghawar Field, Saudi Arabia: evidence

from petrographic and geochemical constraints. *Journal of Sedimentary Research* 75(3): 476-491.

Tariq, M.A., Abid, Q.Z. (1993). Geological map of Pakistan (Scale 1:1,000,000). Geological Survey of Pakistan.

Tucker, M.E. (1993). Carbonate diagenesis and sequence stratigraphy, *Sedimentology Review*, 1: 51-72.

Tucker, M.E., Bathurst, R.G. (2009). Carbonate diagenesis. John Wiley & Sons.

Tucker, M.E., Wright, V.P. (1990). Carbonate Sedimentology. Blackwell Scientific Publications: Oxford.

Ullah, N., Saboor, A., Ahmad, W., Haneef, M., Hussain, M.S., Jalil, R., Ullah, Z. (2016). Microfacies, diagenetic fabric and depositional environment of Middle Jurassic Samana Suk Limestone, Lower Salhad, Abbottabad Pakistan. 2nd International conference on: Sustainable Utilization of Natural Resource, National Centre of Excellence in Geology, University of Peshawar, Pakistan

Wadood, B., Aziz, M., Ali, J., Khan, N., Wadood, J., Khan, A., Ullah, M. (2021). Depositional, diagenetic, and sequence stratigraphic constrains on reservoir characterization: a case study of middle Jurassic Samana Suk Formation, western Salt Range, Pakistan. *Journal of Sedimentary Environments* 6:131-147.

Wadood, B., Khan, S., Li, H., Liu, Y., Ahmad, S., Jiao, X. (2021). Sequence stratigraphic framework of the Jurassic Samana Suk carbonate formation, North Pakistan: Implications for reservoir potential. *Arabian Journal for Science and Engineering* 46(1): 525-542.

Warren, J. (2000). Dolomite: occurrence, evolution and economically important associations, *Earth-Science Reviews* 52(1-3): 1-81.

Weijermars, R. (1989). Global tectonics since the breakup of Pangea 180 million years ago: evolution maps and lithospheric budget. *Earth-Science Reviews* 26(1-3): 113-162.

Xu, W.L., Li, J.Z., Liu, X.S., Li, N.X., Zhang, C.L., Zhang, Y.Q. (2021). Accumulation conditions and exploration directions of Ordovician lower assemblage natural gas, Ordos Basin, NW China. *Petroleum Exploration and Development* 48 (3): 641–654.

Yeats, R.S., Hussain, A. (1987). Timing of structural events in the Himalayan foothills of northwestern Pakistan. *Geological society of America bulletin* 99(2): 161-176.

Zhemchugova, V.A., Evdokimov, N.V., Poort, J., Akhmanov, G.G. (2020). Lower Permian Carbonate Buildups in the Northern Timan–Pechora Basin as the Main Hydrocarbon Exploration Object. *Lithology and Mineral Resources* 55: 245-260.